



AFRL-RX-WP-TP-2012-0374

**THEORETICAL AND EXPERIMENTAL
INVESTIGATIONS ON THE MECHANISM OF
CARBOTHERMAL REDUCTION OF ZIRCONIA
(PREPRINT)**

**Anchal Sondhi, Carl Morandi, Richard F. Reidy, and Thomas W. Scharf
University of North Texas**

**August 2012
Interim**

Approved for public release; distribution unlimited.

See additional restrictions described on inside pages

STINFO COPY

**AIR FORCE RESEARCH LABORATORY
MATERIALS AND MANUFACTURING DIRECTORATE
WRIGHT-PATTERSON AIR FORCE BASE, OH 45433-7750
AIR FORCE MATERIEL COMMAND
UNITED STATES AIR FORCE**

REPORT DOCUMENTATION PAGE					Form Approved OMB No. 0704-0188	
<p>The public reporting burden for this collection of information is estimated to average 1 hour per response, including the time for reviewing instructions, searching existing data sources, gathering and maintaining the data needed, and completing and reviewing the collection of information. Send comments regarding this burden estimate or any other aspect of this collection of information, including suggestions for reducing this burden, to Department of Defense, Washington Headquarters Services, Directorate for Information Operations and Reports (0704-0188), 1215 Jefferson Davis Highway, Suite 1204, Arlington, VA 22202-4302. Respondents should be aware that notwithstanding any other provision of law, no person shall be subject to any penalty for failing to comply with a collection of information if it does not display a currently valid OMB control number. PLEASE DO NOT RETURN YOUR FORM TO THE ABOVE ADDRESS.</p>						
1. REPORT DATE (DD-MM-YY) August 2012		2. REPORT TYPE Technical Paper		3. DATES COVERED (From - To) 1 July 2012 – 1 August 2012		
4. TITLE AND SUBTITLE THEORETICAL AND EXPERIMENTAL INVESTIGATIONS ON THE MECHANISM OF CARBOTHERMAL REDUCTION OF ZIRCONIA (PREPRINT)				5a. CONTRACT NUMBER FA8650-08-C-5226		
				5b. GRANT NUMBER		
				5c. PROGRAM ELEMENT NUMBER 62102F		
6. AUTHOR(S) Anchal Sondhi, Carl Morandi, Richard F. Reidy, and Thomas W. Scharf (University of North Texas)				5d. PROJECT NUMBER 4347		
				5e. TASK NUMBER		
				5f. WORK UNIT NUMBER LM114100		
7. PERFORMING ORGANIZATION NAME(S) AND ADDRESS(ES) University of North Texas Corner of Avenue C Chestnut Denton, TX 76203				8. PERFORMING ORGANIZATION REPORT NUMBER		
9. SPONSORING/MONITORING AGENCY NAME(S) AND ADDRESS(ES) Air Force Research Laboratory Materials and Manufacturing Directorate Wright-Patterson Air Force Base, OH 45433-7750 Air Force Materiel Command United States Air Force				10. SPONSORING/MONITORING AGENCY ACRONYM(S) AFRL/RXCM		
				11. SPONSORING/MONITORING AGENCY REPORT NUMBER(S) AFRL-RX-WP-TP-2012-0374		
12. DISTRIBUTION/AVAILABILITY STATEMENT Approved for public release; distribution unlimited. Preprint to be submitted to Journal of the American Ceramic Society.						
13. SUPPLEMENTARY NOTES The U.S. Government is joint author of this work and has the right to use, modify, reproduce, release, perform, display, or disclose the work. PA Case Number and clearance date: 88ABW-2012-3560, 22 June 2012. This document contains color.						
14. ABSTRACT Zirconium carbide (ZrC) is an important ultra high temperature ceramic due to its refractory properties. It is commonly synthesized via carbothermal reduction of zirconia above 1657 degrees Celsius according to the reaction $ZrO_2(s) + 3C(s) + 2CO(g)$. Contrary to this reaction, prior research indicates that carbon monoxide (CO) is the responsible species for carburizing ZrO_2 to form ZrC. To explore this reaction pathway, investigations were performed by making two mixed phase pellets with 3 mol% yttria-stabilized zirconia (YSZ) and graphite. Both had an upper half made of YSZ. The lower half of one sample consisted of finely mixed YSZ and graphite powder whereas the other was pure graphite. Similar experiments were conducted with sintered YSZ pellets on top. After heat treatment at 1800 degrees Celsius, X-ray diffraction analysis revealed higher ZrC conversion for the YSZ pellet face in direct contact with pure graphite. This contradicts previous work as one would assume higher ZrC yield for YSZ pellet in direct contact with YSZ/graphite mix as they produce more CO upon reaction. Lastly, diffusional experiments showed conversion to be highly...						
15. SUBJECT TERMS carbothermal reduction, carbon diffusion, ultra high temperature ceramic, zirconium carbide, yttria-stabilized zirconia						
16. SECURITY CLASSIFICATION OF:			17. LIMITATION OF ABSTRACT: SAR	NUMBER OF PAGES 32	19a. NAME OF RESPONSIBLE PERSON (Monitor) Jaimie Tiley 19b. TELEPHONE NUMBER (Include Area Code) N/A	
a. REPORT Unclassified	b. ABSTRACT Unclassified	c. THIS PAGE Unclassified				

Theoretical and Experimental Investigations on the Mechanism of Carbothermal Reduction of Zirconia

Anchal Sondhi, Carl Morandi,[‡] Richard F. Reidy[£] and Thomas W. Scharf

Department of Materials Science & Engineering and Institute for Science and Engineering
Simulation (ISES)

University of North Texas

Denton, TX 76207 USA

Abstract

Zirconium carbide (ZrC) is an important ultra high temperature ceramic due to its refractory properties. It is commonly synthesized via carbothermal reduction of zirconia above 1657°C according to the reaction $\text{ZrO}_2(\text{s}) + 3\text{C}(\text{s}) \rightarrow \text{ZrC}(\text{s}) + 2\text{CO}(\text{g})$. Contrary to this reaction, prior research indicates that carbon monoxide (CO) is the responsible species for carburizing ZrO_2 to form ZrC. To explore this reaction pathway, investigations were performed by making two mixed phase pellets with 3 mol% yttria-stabilized zirconia (YSZ) and graphite. Both had an upper half made of YSZ. The lower half of one sample consisted of finely mixed YSZ and graphite powder whereas the other was pure graphite. Similar experiments were conducted with sintered YSZ pellets on top. After heat treatment at 1800°C, X-ray diffraction analysis revealed higher ZrC conversion for the YSZ pellet face in direct contact with pure graphite. This contradicts previous work as one would assume higher ZrC yield for YSZ pellet in direct contact with YSZ/graphite mix as they produce more CO upon reaction. Lastly, diffusional experiments

showed conversion to be highly localized to a depth of $\sim 20\mu\text{m}$. This is in close agreement with calculations for carbon diffusion in YSZ based on a diffusion coefficient (D) = $3 \times 10^{-14} \text{ m}^2/\text{sec}$, which confirms solid-solid reaction rather than solid-gas reaction.

Keywords: Carbothermal reduction, Carbon diffusion, Ultra high temperature Ceramic, Zirconium Carbide, Yttria-stabilized zirconia

[¥]Currently at The Department of Materials Science and Engineering, The Pennsylvania State University

[£]Author to whom correspondence should be addressed. e-mail:reidy@unt.edu

1. Introduction

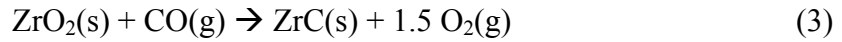
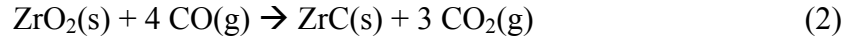
Zirconium carbide is known for its high melting temperature, 3400-3540 °C, high hardness, 2100 Knoop, and high modulus of elasticity, 380 GPa.¹ These properties enable it to be used in cutting tools, as a refractory material and in composites to impart high strength. It has also found applications in electronic devices² and as a low neutron absorbing material in the nuclear industry.³

Carbothermal reduction is a common chemical process practiced commercially for the synthesis of many non-oxide ceramic powders. Zirconium carbide powders have long been produced by using carbothermal reduction under various conditions and atmospheres.^{4,5} The mechanism and species involved leading to carbide conversion has been studied since the early 1980s when Vodop'yanov et. al.^{6,7} reported that at high temperatures zirconia (ZrO₂) reacts with carbon monoxide (CO) to form carbides on the surface of oxides under non-vacuum conditions. In experiments conducted in inert atmospheres⁸, ZrO₂ reacts with CO to form an oxycarbide phase, ZrC_{0.9-x}O_x (x=0.04-0.08) that subsequently forms ZrC.⁹ Absent from these studies is the dependence of CO partial pressure on this reaction. CO occurs as a reaction product during carbothermal reduction of zirconia at temperatures of 1657°C and above¹⁰ according to



This reaction shows that the CO available for reaction with zirconia is dependent on the prior carbothermal reduction of ZrO₂. Moreover, CO is a larger species than C which precludes its diffusion in zirconia.

Thermodynamic reactions involving CO and ZrO₂ indicate that ZrC is unlikely to form from these reactants. Fig.1 shows change in Gibbs free energy (ΔG) plots for two different reactions (Equations 2 and 3) between ZrO₂ and CO:



The ΔG values are highly positive for a large temperature range confirming that under atmospheric pressure CO is unlikely to react with ZrO₂ to form ZrC.^{11,12} Reactions (2) and (3) can go in the forward direction only (i.e., have negative ΔG values) under non-equilibrium conditions. These values are governed by the following equation,

$$\Delta G = \Delta G^0 + RT \ln K \quad (4)$$

where ΔG^0 is change in Gibbs free energy at standard state, R is the gas constant, T is the absolute temperature, and K is the reaction rate constant. Fig. 1 shows ΔG^0 is always positive for both reactions. Thus for ΔG to be negative, $\Delta G^0 < -RT \ln K$. Therefore, unless the partial pressures of CO are very high (1.91×10^9 atm at 298K for reaction (2)), CO will not convert ZrO₂ to ZrC. Moreover, under equilibrium conditions and unit activity of solids in reaction (1), partial pressure of CO is calculated to be 3.98 atm at 1800 °C. This makes it extremely difficult for CO to initiate any ZrO₂ to ZrC transformation.

In many reactions such as



varied ratios of CO, CO₂ and O₂ can result in activity of carbon greater than one. Consequently, carbon would start depositing from atmosphere. Our system has a partial pressure of O₂ at

$\sim 9.52 \times 10^{-7}$ atm. A quick analysis would reveal that unless the partial pressure of O_2 is not less than $\sim 3.09 \times 10^{-14}$ atm, the activity of graphite would not exceed a value of one according to reaction (5).^{11,12} Therefore, the motivation of this study is to determine the mechanism for carbothermal reduction of ZrO_2 into ZrC .

2. Experimental Procedure

2.1 Sample preparation

A composite pellet system was designed that consisted of two parts: upper and lower halves which were made separately by die pressing powders to form pellets. The YSZ powder was manufactured by Tosoh Corporation under product name TZ-3Y-E. The 3 mol% YSZ exhibited specific area of $15.2 \text{ m}^2/\text{g}$ and crystallite size of $\sim 26 \text{ nm}$. The graphite powder (300 mesh size) was produced by Alfa Aesar. The motivation behind constructing a composite system was to use the bottom half of the pellet as a source of CO and/or C for reactions to occur into and within the top half. Fig. 2 shows the two composite systems, MP2 and P3, and their sintered counterparts, MP2s and P3s. MP2 consisted of a bottom half made up of YSZ and graphite mixed using a mortar and pestle in a molar ratio of 1:3.3. This powder blend was then die pressed at uniaxial pressure of 5 ksi to form a cylindrical shaped pellet. The P3 die pressed cylindrical pellet consisted of a bottom half made only from 0.25 gm graphite powder. Both top halves were made up of 1gm of YSZ powder again die pressed to cylindrical pellet of density $\sim 2.94 \text{ g/cm}^3$. In MP2s and P3s samples, the YSZ was sintered after die pressing. The sintering temperature-time profile is shown in Fig. 3.

2.2 Carbothermal reduction heat treatments

All heat treatments were done under flowing helium in a Thermal Technology graphite furnace (Model 1000-2560-FP20). Prior to heat treatments, the chamber was pumped down to $\sim 10^{-6}$ torr base pressure and then flushed with research grade He. Samples were heated to a temperature of 1800°C under flowing He by using the procedure shown in Fig. 4. This involved a ramp up from room temperature to 1350°C at a rate of 300°C/hr, from 1350°C to 1650°C a rate of 1800°C/hr, from 1650°C to 1800°C at a rate of 300°C/hr, followed by a dwell of 30 minutes and cooling down to 20°C at 300°C/hr.

2.3 Characterization

Cu-K α X-ray diffraction (XRD) was done using a Rigaku Ultima III diffractometer. Scans were acquired from top and bottom halves/faces of all the pellets before and after heat treatments. These were then analyzed for the phases present and their respective mole fractions. Peak identification corresponding to YSZ, graphite and zirconium carbide were done using JCPDS files nos. 01-070-4426, 01-071-4630 and 01-073-0477, respectively. MDI Jade software was used for peak identification and Reitveld refinement on all XRD scans to obtain molar percentages of the various phases.

3. Results and Discussion

3.1 Characterization of pellets before and after carbothermal reduction heat treatment

XRD determined that the 3 mol% YSZ raw powder consisted of tetragonal and monoclinic zirconia phases shown in Fig. 5. The basic aim behind designing the four composite pellet systems was to control the relative amounts of CO and C diffusing into their respective YSZ top halves. Based on Reaction (1), the MP2 pellet would form ZrC and liberate CO at $T > 1657^{\circ}\text{C}$.

This CO along with C is then available to react with the top half of the pellet. Due to a mixed bottom half in MP2, CO, in principle, is the primary diffusional species. P3 has a bottom half composed only of graphite. Thus, C, in principle, would be the primary species diffusing into its top half. Therefore, CO generation due to the YSZ and graphite reaction at the top and bottom interface would be considerably less in P3 compared to the MP2 pellet. As a result, C would be a more abundant diffusional species in P3 than CO. The sintered pellets, MP2s and P3s, have the same bottom halves as MP2 and P3, respectively, but the YSZ top halves are sintered to 98% of theoretical density. CO gas diffusion would thus be limited in sintered YSZ since there is negligible porosity limiting diffusion of the larger CO molecule. Like in MP2, the primary species available for reaction with ZrO_2 in MP2s is CO while C is much less abundant. In P3s the primary abundant species for diffusion is C whereas CO would be the minor species.

At the carbothermal reduction heat treatment temperature of 1800°C , C and CO can diffuse from the bottom half of a pellet (source) into its respective top half (sink). Even with increased mobility of these species, carbothermal reduction will occur only at temperatures where reaction (1) has negative values of the Gibbs free energy. The bottom half of each pellet serves as a carbon source for the respective YSZ top half. As previously mentioned, MP2 and P3 have different dominant carbon species available to react with the top halves. MP2 has gaseous CO in abundance while P3 provides only C as a reactant, at least initially. If available, the gaseous species can react with both faces and sides of the YSZ top half. However, in the P3 pellet, solid carbon is in contact with YSZ and should result in a more solid diffusion based reaction.

To differentiate amongst these possible reactions, separate XRD scans were acquired from the bottom and top halves. Fig. 6(a) shows XRD results acquired from the bottom half of MP2. There are no peaks corresponding to YSZ confirming full conversion to ZrC. Although not

shown, MP2s exhibited the same XRD peaks. Conversely, XRD results on P3, shown in Fig. 6(b), and P3s (not shown) exhibited only graphite peaks with no peaks corresponding to YSZ or ZrC. To characterize the top halves of the MP2, P3, MP2s, and P3s pellets, both its top and bottom faces were analyzed according to the procedure shown in Fig. 7. The corresponding XRD scans in Fig. 8 all show the presence of tetragonal ZrO₂ and ZrC in varying percentages, but with no presence of monoclinic ZrO₂. In Table 1, quantitative Reitveld refinement analyses show maximum ZrC conversion occurred for the bottom face of P3 pellet followed by the P3s, MP2 and MP2s pellets. The reason for this trend is because the P3 pellets are a greater source of C, and, thus show a larger amount of ZrC formation. Meanwhile, the sintered samples show less ZrC formation than their un-sintered counterparts because sintering severely limits exposed interior surfaces as potential reaction sites.

3.2 Bulk diffusion of C in YSZ pellets

The carbon diffusion coefficient in zirconia has been reported to be six orders of magnitude smaller than oxygen self-diffusion¹³. This would indicate several orders of magnitude difference in diffusivity between C and CO through YSZ due to the gaseous nature of CO. Based on the recent work of Vykhodets *et al*¹³ and utilizing their data, the diffusion coefficient of C in YSZ at 1800 °C is calculated to be 3×10^{-14} m²/sec. Using Fick's second law and this diffusion coefficient, the effective diffusion length of C in YSZ can be approximated to 25 µm for 0.5 hour at 1800°C (calculated plots shown in Fig. 9). According to these results at distances greater than 25 µm there should not be any ZrC formation due to lack of diffusing carbon. To confirm the presence or absence of ZrC experimentally, the top halves of MP2, P3, MP2s, and P3s were sliced radially close to half their heights, shown in Fig. 10. After slicing, XRD scans were acquired from the exposed faces, namely Face A and Face B while keeping the X-ray beam close

to the geometric center. Fig. 11 shows the XRD scans obtained from Face A and Face B for all the pellets. None of the scans show the dominant ZrC (111) peak at $2\theta=33.2^\circ$. On the contrary, all the peaks correspond to YSZ (monoclinic and tetragonal phases) confirming that no ZrC formed in the center, at least to these 1.5-2 mm depths. Fig. 9 theoretically shows for longer diffusion times of 1 hour (circles) to 1.5 hours (triangles), C cannot diffuse past 50 μm distance. These results further confirm that carbothermal reduction is more C driven than CO driven due to its slow diffusional nature. X-ray penetration depth calculations indicate that the diffraction analysis only examines approximately the first 16-20 microns of ZrO_2/ZrC .

3.3 Surface Diffusion of C on YSZ pellets

As mentioned earlier, the bottom half of MP2 acts as a strong source of CO and a weak source of C for diffusion into the top half. In contrast, P3 acts as a strong C source and a weak CO source for its top half. In principle, during the course of the carbothermal reduction reaction, it is feasible that CO as a reaction product can be liberated from the sample and potentially form a sheath around the top YSZ pellet leading to radially inward diffusion. Similarly, C due to being a small and relatively mobile species can also diffuse to the top from surface sites on the pellet edges. These pathways can possibly cause a gradient in the amount of YSZ converted to ZrC along the sides of the pellet in addition to the aforementioned bulk transformations occurring at respective bottom and top faces. Given the differences between gaseous and surface diffusion rates, one would expect that surface diffusion would have more observable time dependence. The physical inspection of the top halves after heat treatment showed color changes from bright white to grey to black indicating reactions occurred at the pellets' frustum.

Examination of these surface effects is important to understand details of the diffusion mechanism(s). To this end, a series of XRD spot scans were performed on one of the sliced faces (Face A or Face B) of the MP2s and P3s pellets. These spot scans, when stitched together, form a line that connects the pellet edge to its center as shown in Fig. 12. Such a line scan can reveal a possible transition from ZrC to YSZ along the radial direction of the pellet. These XRD acquisitions, done using rectangular X-ray beam cross-sections, were made spatially large enough to cover considerable areas near the edge and center of the pellet's face.

XRD line scan results obtained from this procedure are shown in Fig. 13(a) for MP2s and Fig. 13(b) for P3s. For both pellets, only YSZ peaks were detected with no evidence of ZrC reflections on all the XRD scans obtained from points 1 to 8, albeit within the XRD spatial detection limit. This confirms that any surface diffusion occurring is significantly less than the previously observed bulk diffusion in the top and bottom faces of the MP2, P3, MP2s, and P3s top halves. Corresponding optical images of the X-ray spot streaks superimposed on actual samples are shown for MP2s (Fig. 13(c)) and P3s (Fig. 13(d)).

3.4 Discussion on mechanism of carbothermal reduction of zirconia

During the carbothermal reduction heat treatment, the bottom face of the MP2 top half (YSZ) is exposed to more CO than P3 because of its mixed ZrO₂ and C bottom half. Based on previous research^{6-9, 14} where CO is thought to be the reaction driver for ZrC conversion, the bottom face of the MP2 top half should produce more ZrC formation than P3. However, it was determined that P3 bottom face exhibits significantly more ZrC conversion (70%) than MP2 (23%). The pellet systems studied have CO and C as the only likely species capable of carburizing YSZ to ZrC. Since MP2 and P3 have porous top halves, $\sim 2.94\text{g/cm}^3$, both species can diffuse through

pores making it difficult to conclude which is the dominating species driving carbide formation. To study this effect, sintered versions of these samples, P3s and MP2s, were exposed to the same heat treatments and carbonaceous exposures as their porous counterparts. In both sintered samples, the top and bottom faces still show ZrO_2 to ZrC conversion, albeit less mole percent than the corresponding non-sintered pellets. These sintered YSZ top halves should, in principle, restrict or minimize any gaseous CO diffusion through them and only react through direct contact or gaseous species emanating from the lower halves. However, carbon because of its very small size can diffuse via grain boundaries, interstitial sites and lattice defect sites. Thus, reduction of YSZ to ZrC is still observed in the sintered P3s and MP2s pellets.

Moreover, diffusion measurements¹³ show that kinetics of carbon diffusion in zirconia is rather slow. Thus, any YSZ to ZrC conversion occurring because of carbon will be highly localized. Experimental XRD results on Face A and B of the top halves confirms this since no ZrC was detected. In support of this, calculated X-ray depth penetration using procedure in ref. 15 is less than 20 μm on bottom faces of all the pellets. This is in agreement with results and analysis from Vykhodets et al.¹³ where carbon can diffuse only to depths of $\sim 25 \mu\text{m}$ at 1800°C , shown in Fig. 9. This effectively means that carbon diffusion in YSZ is so slow that it causes the diffusion front to extend to similar depths as that of the conversion front of ZrO_2 to ZrC transformation.

4. Summary and Conclusions

Experiments and calculations were performed to determine carbothermal reduction mechanisms and whether CO is the dominant species driving the ZrO_2 to ZrC conversion. A series of experiments using pellet systems were conducted in which controlled amounts of CO and C were exposed to YSZ, and the reaction products were analyzed to confirm the reaction driver. If CO is

the source of C for ZrC formation then the sample with the most available CO, MP2, would exhibit the highest conversion; however, this was not observed. Instead, P3, which has a bottom half of graphite acts as a weak source of CO, shows maximum ZrC formation at the interface between top and bottom half due to solid-solid reaction of zirconia and graphite. In addition, top halves of MP2 and P3 undergo sintering and reaction at the same time. This restricts CO diffusion through the bulk as the top pellets are sintered to ~77% of theoretical density of zirconia.. To form ZrC, a carbonaceous species must transport into ZrO₂, thus, C is a much more likely species to diffuse through a sintered sample than CO. In support of this mechanism, theoretical calculations indicate partial pressures of CO needed to drive zirconium carbide formation from zirconia are far beyond the environment in the reaction furnace. Since most of the processing is done under atmospheric pressure, so as to avoid capital investments and safety issues, formation of ZrC by reaction between ZrO₂ and CO appears less likely than carbon diffusion.

In addition, carbon diffusion in zirconia is slow even at elevated temperatures. Thus any ZrC formation is highly localized as seen experimentally in all the top halves as well as theoretically based on diffusion depth calculations. These results indicate carbothermal reduction to be C driven as CO would be expected to be orders of magnitude faster than C and cause unlocalized diffusion (within the sample pores). Based on the above, carbothermal reduction of zirconia is more dependent on solid-solid reaction than gas-solid reaction, which is in disagreement with previous research findings that suggest carbothermal reduction of zirconia to be only a CO driven reaction mechanism.

Acknowledgments

The authors would like to acknowledge the financial support from the U.S. Air Force Research Laboratory (AFRL, ISES Contract No. FA8650-08-C-5226). We also acknowledge the use of the XRD facilities at the UNT Center for Advance Research and Technology (CART).

References

1. C.A. Daniels, "Data Section"; pp. 210-211 in *Ceramics: Structure and Properties*. Abyss Books, Washington, D.C., 2002.
2. G. Montel, A. Lebugle and H. Pastor. "Manufacture of Materials Containing Refractory Borides, Carbides, and Nitrides, and Their Application in Electronics and Electrical Engineering; Elaboration et Applications A L'Electronique et a L'Electrotechnique des Materiaux Contenant des Borures, Carbures et Nitrides Refractaires," *Revue Internationale des Hautes Temperatures et des Refractaires*, 16, 95-124 (1979).
3. G.V. Samsonov, "Properties index" pp. 336-7 in *Plenum Press Handbook of High Temperature Materials*, No. 2: Properties Index, Plenum Press, New York, NY, 1964.
4. J.I. Kroschwitz and A. Seidel, "Ceramics, Industrial Hard"; pp. 694 in *Kirk-Othmer encyclopedia of chemical technology*, Vol. 4; Wiley-Interscience, Hoboken, N.J., 2004; 2006.
5. J.I. Kroschwitz and A. Seidel, "Zirconium and Zirconium Compounds"; pp. 640 in *Kirk-Othmer encyclopedia of chemical technology*, Vol. 26; Wiley-Interscience, Hoboken, N.J., 2004; 2006.
6. A.G. Vodop'yanov, *Izv. Akad. Nauk SSSR, Metally*, **5**, (1981), 37.

7. A.G. Vodop'yanov, G.N. Kozhevnikov, S.V. Baranov and S.V. and Zhidovinova. *Izv. Akad. Nauk SSSR, Metally*, **3**, (1986), 5.
8. A. Maitre and P. Lefort. "Solid state reaction of zirconia with carbon," *Solid State Ionics*, **104**, 109-22 (1997).
9. L.-. Berger, W. Gruner, E. Langholf and S. Stolle. "On the mechanism of carbothermal reduction processes of TiO_2 and ZrO_2 ," *International Journal of Refractory Metals and Hard Materials*, **17**, 235-43 (1999).
10. A.W. Weimer, *Carbide, nitride and boride materials synthesis and processing*; Chapman & Hall, London [u.a.], 1997.
11. C.W. Bale, E. Bélisle, P. Chartrand, et al. "FactSage thermochemical software and databases — recent developments," *Calphad*, **33**, 295-311 (2009) <<http://www.sgte.org/reacweb.htm>>
12. M.W. Chase and United States National Bureau of Standards. *JANAF thermochemical tables*; American Chemical Society ; American Institute of Physics for the National Bureau of Standards, Washington, D.C.; New York, 1986.
13. V. Vykhodets, T. Kurennikh, A. Kesarev, et al. "Diffusion of insoluble carbon in zirconium oxides," *JETP Letters*, **93**, 5-9 (2011).
14. W. Gruner, S. Stolle, L.-. Berger and K. Wetzig. "A new experimental approach for accelerated investigations of carbothermal reactions," *International Journal of Refractory Metals and Hard Materials*, **17**, 227-34 (1999).
15. B.D. Cullity and S.R. Stock, "Diffraction II: Intensities of Diffracted Beams"; pp. 152-154 in *Elements of x-ray diffraction*; Prentice Hall, Upper Saddle River, NJ, 2001.

Table 1. Approximate mole percentages of tetragonal zirconia and zirconium carbide on top and bottom faces of respective pellet top halves.

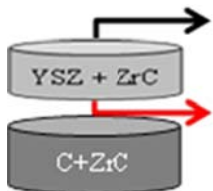
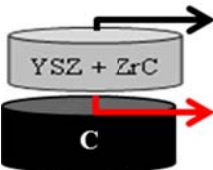
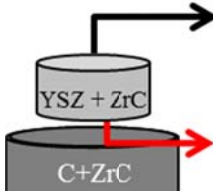
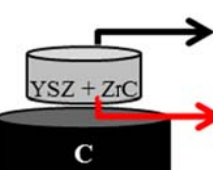
Sample Name	Mole Percentages
MP2 	Top face- 42% ZrC
	Bottom face- 23% ZrC
P3 	Top face- 45% ZrC
	Bottom face- 74% ZrC
MP2s 	Top face- 15% ZrC
	Bottom face- 18% ZrC
P3s 	Top face- 18% ZrC
	Bottom face- 57% ZrC

Figure Captions

Fig. 1. Graphs showing variation of change in Gibbs free energy (ΔG) as a function of temperature for reactions (2) and (3).

Fig. 2. Schematics of pellets (a) MP2, (b) P3, (c) MP2s, and (d) P3s. Shrinkage seen in top half of MP2s and P3s is due to prior sintering of the YSZ pellet.

Fig. 3. Heat treatment procedure for sintering top halves of P3s and MP2s. Each labeled data point shows corresponding temperature at various hold stages.

Fig. 4. Carbothermal reduction heat treatment procedure for MP2, P3, MP2s and P3s. Numbers next to data points indicate corresponding temperature.

Fig. 5. XRD scans of starting YSZ powder showing primarily tetragonal zirconia with some monoclinic zirconia.

Fig. 6. XRD scans acquired from the bottom halves of (a) MP2 and (b) P3 after carbothermal reduction heat treatment.

Fig. 7. Flowchart showing the methodology in XRD analysis of pellets before and after carbothermal reduction heat treatment. The cloud shape represents powder formed from bottom halves as they decompose after heat treatment.

Fig. 8. XRD data acquired from top halves of (i) bottom face and (ii) top face on (a) MP2, (b) P3, (c) MP2s, and (d) P3s pellets. Table I lists the various amounts of ZrC formed on the faces.

Fig. 9. Variation of carbon concentration as a function of diffusion distance and time at 1800°C. Vertical dotted line shows distance that the X-rays penetrated based on diffraction data acquired from bottom and top faces of MP2, P3, MP2s and P3s top halves.

Fig. 10. Schematics of the methodology of slicing top halves of MP2, P3, MP2s and P3s along with approximate dimensions of original and sliced pellets. Face A and Face B are labeled according to their geometric locations on sliced halves.

Fig. 11. XRD scans from Face A and Face B (Fig. 10) of sliced MP2, P3, MP2s, and P3s top halves. No ZrC peak could be seen in any of the eight acquisitions.

Fig. 12. Schematic of the various points for XRD measurements along the sliced face (A or B) of a top pellet. Rectangular region represents XRD stage on which the pellet rests. The lines denote points 1 to 8 where the XRD scans were obtained: point 1 is on the XRD stage which provides no diffraction, and points 2 to 8 span from the very edge of the pellet to near the pellet center.

Fig. 13. Stacked XRD scans acquired from sliced top halves of (a) MP2s and (b) P3s pellets. No ZrC formation was detected along Points 1 to 8. Point 1 corresponds to region near sample stage and Point 8 corresponds to region near center of the sliced pellet. Optical images showing superimposed images of sliced (c) MP2s and (d) P3s top halves with florescent streaks (denoted by arrows). Florescent streaks were captured separately using same scale as that for sliced sample images.

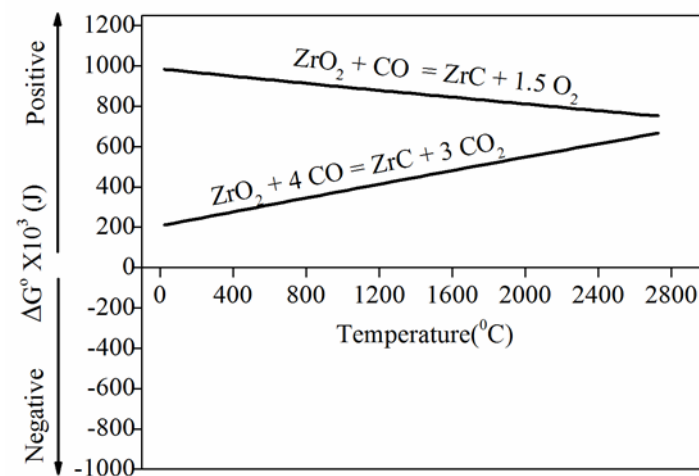


Fig. 1

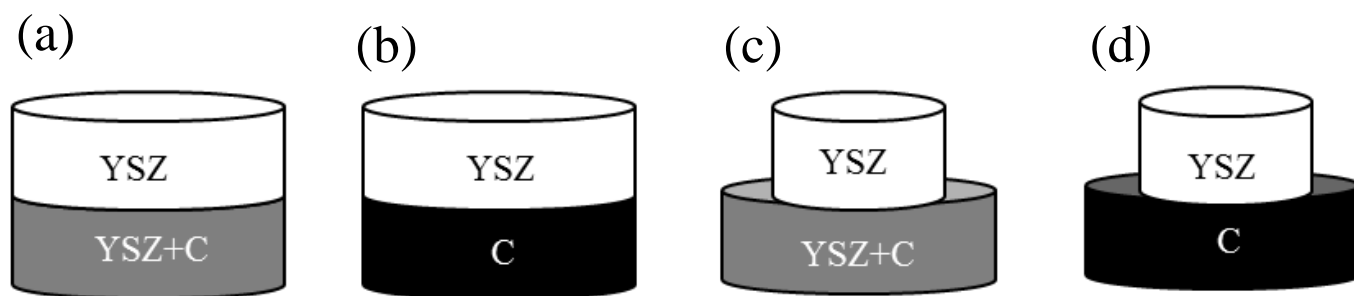


Fig. 2

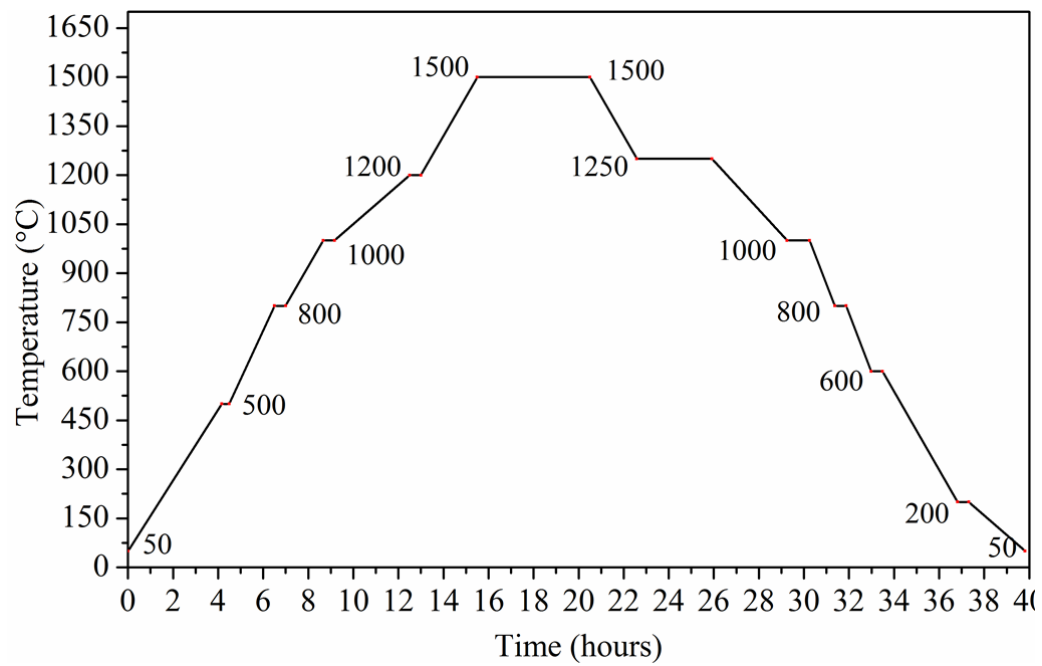


Fig. 3

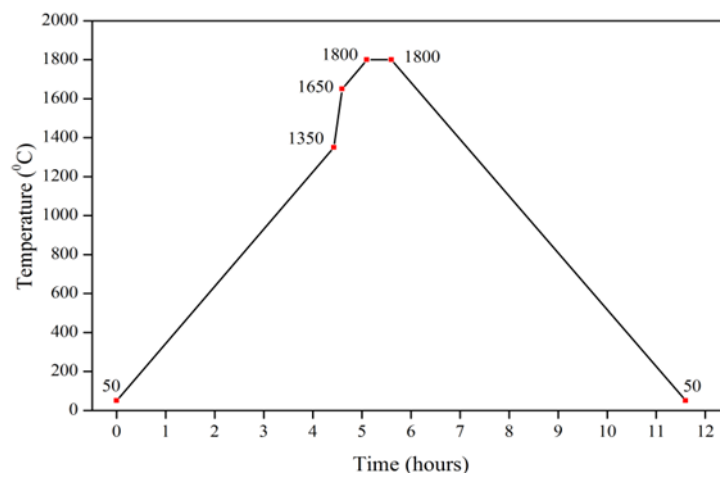


Fig. 4

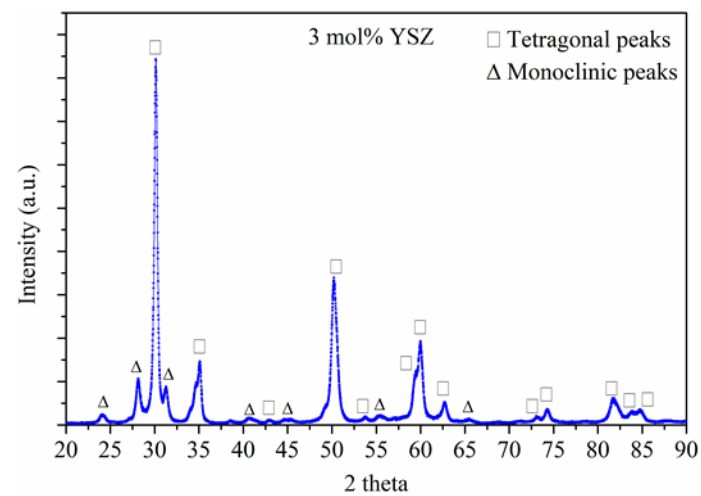


Fig. 5

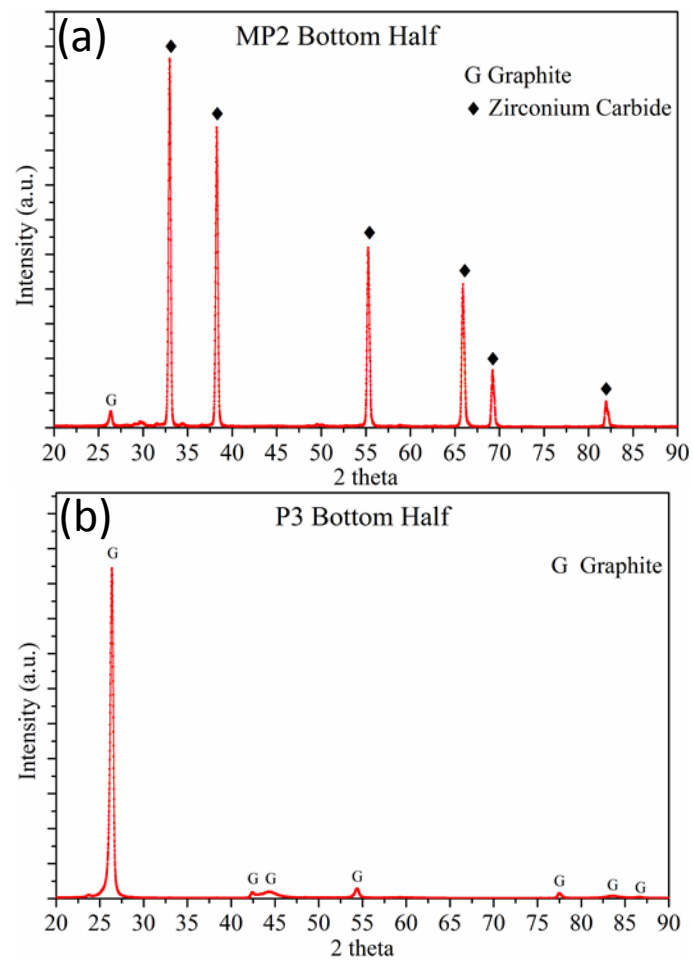


Fig. 6

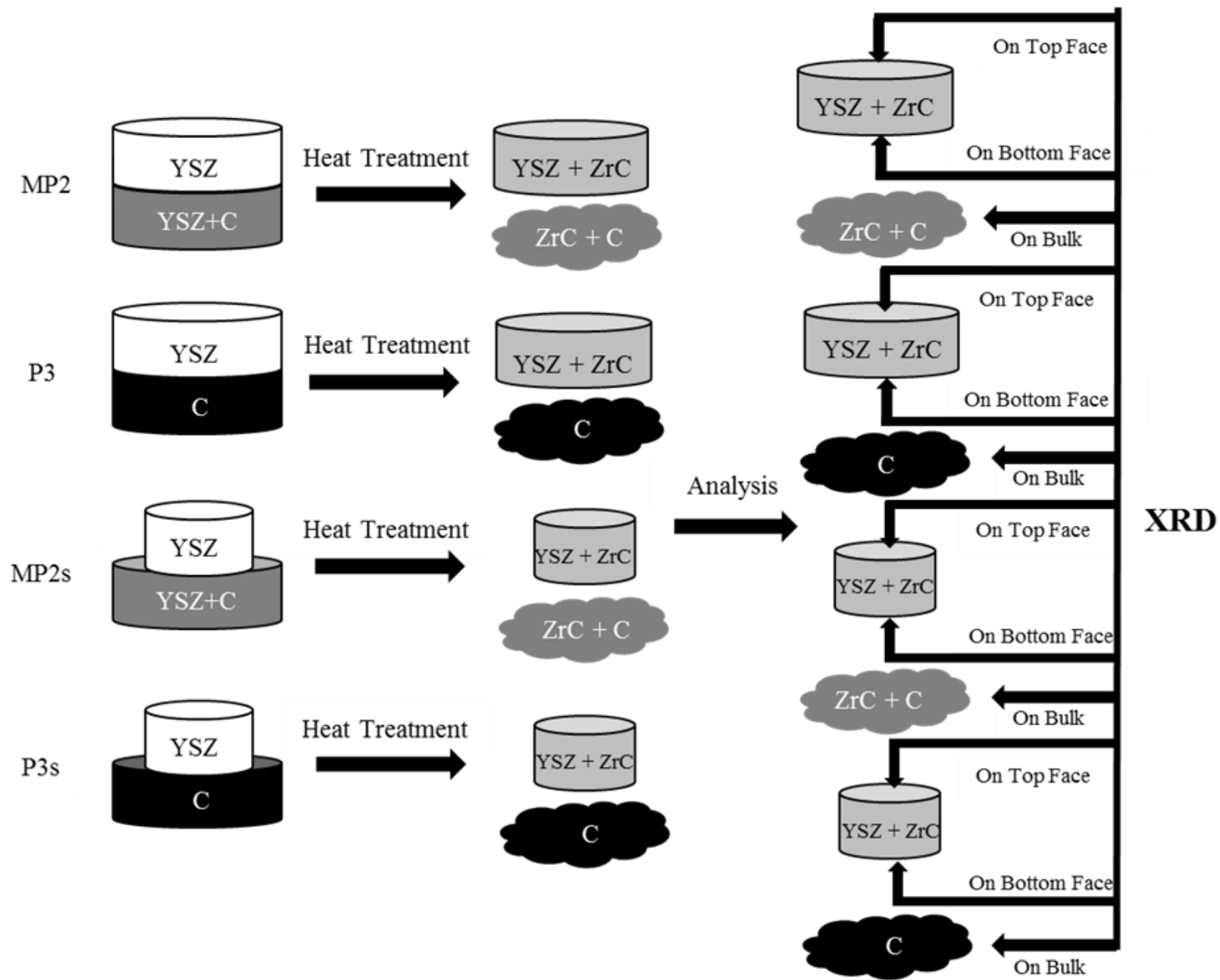


Fig. 7

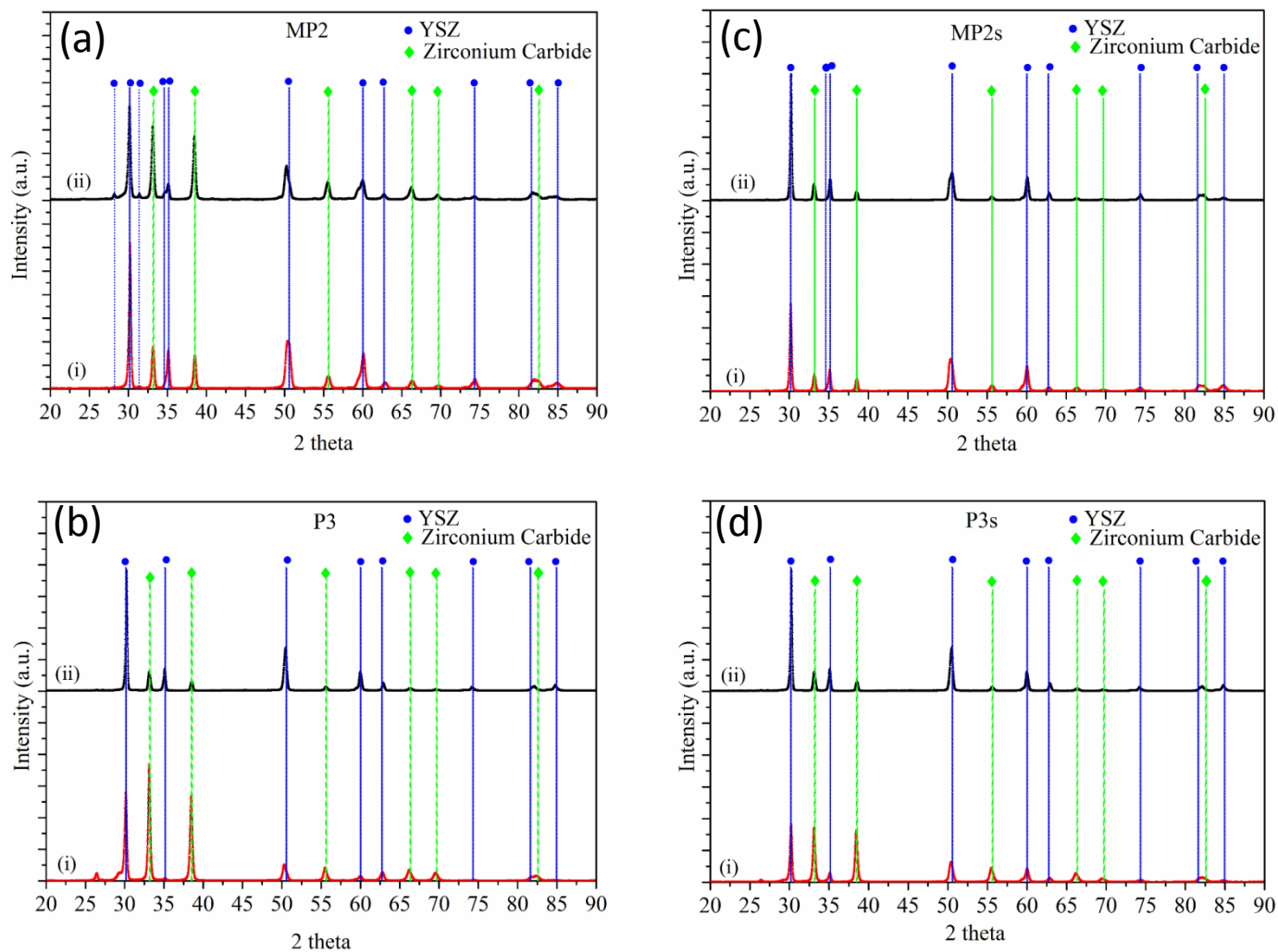


Fig. 8

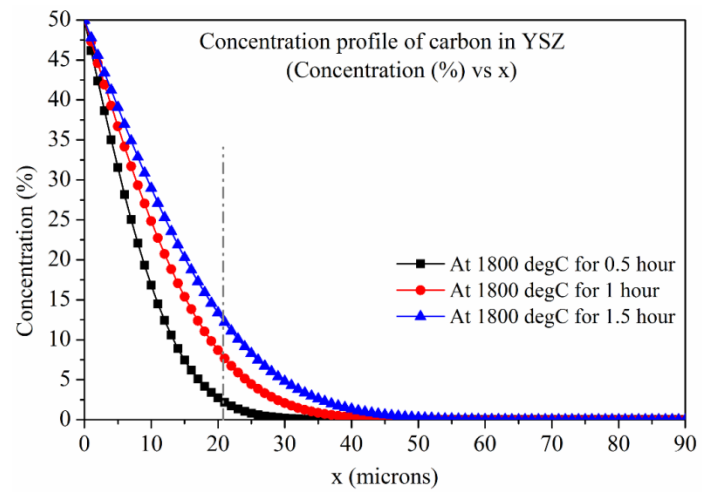


Fig. 9

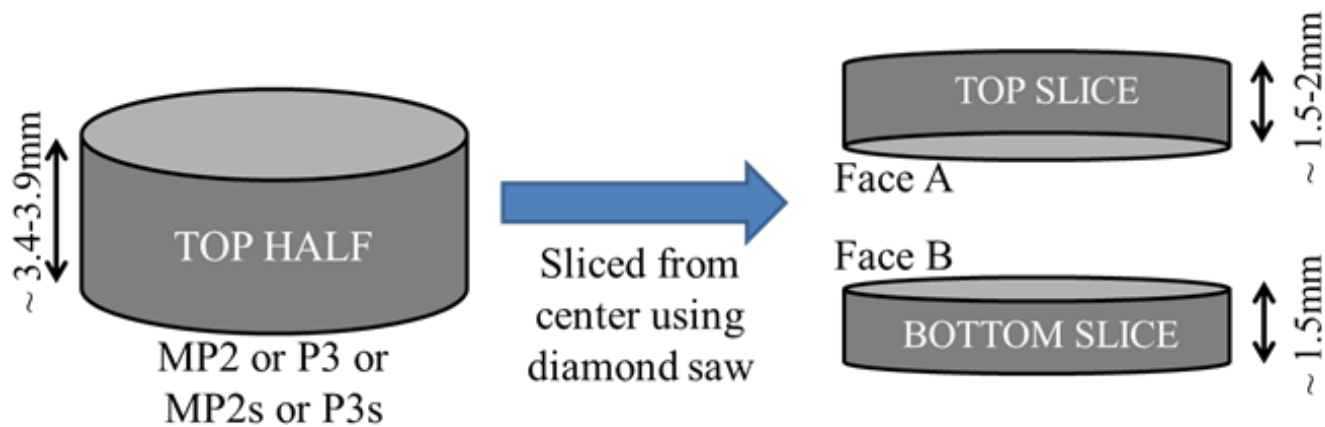


Fig. 10

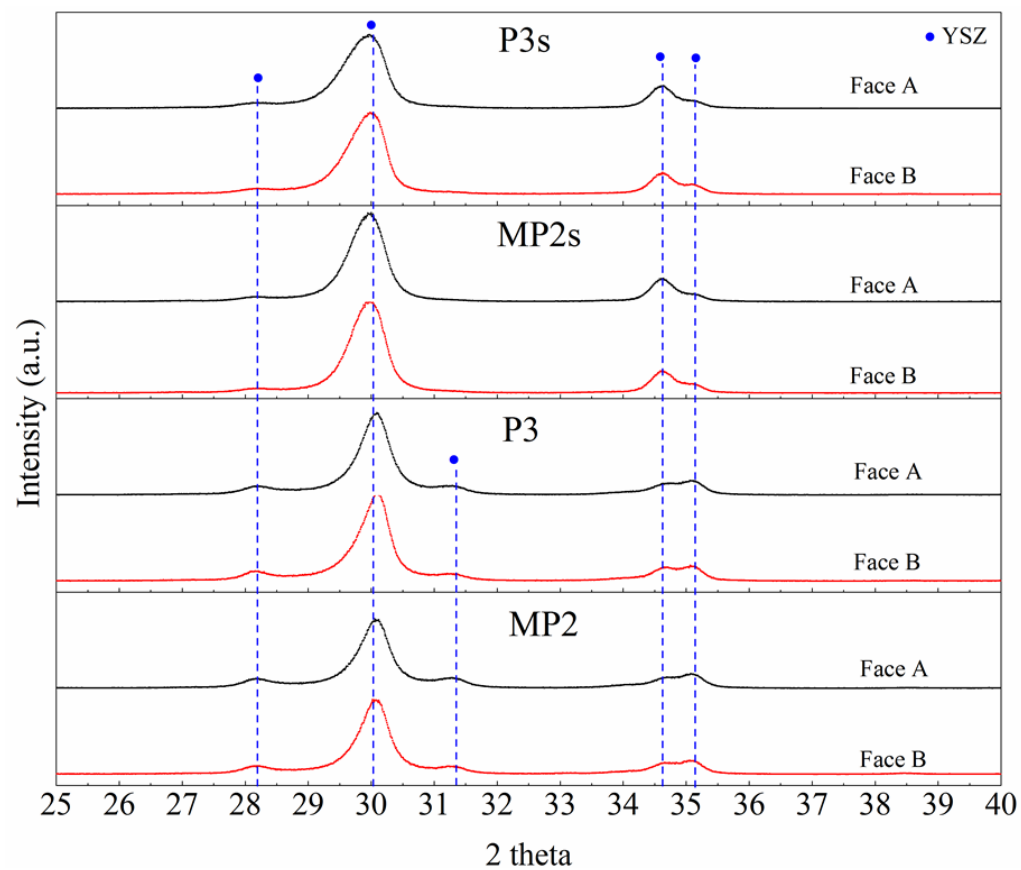


Fig. 11

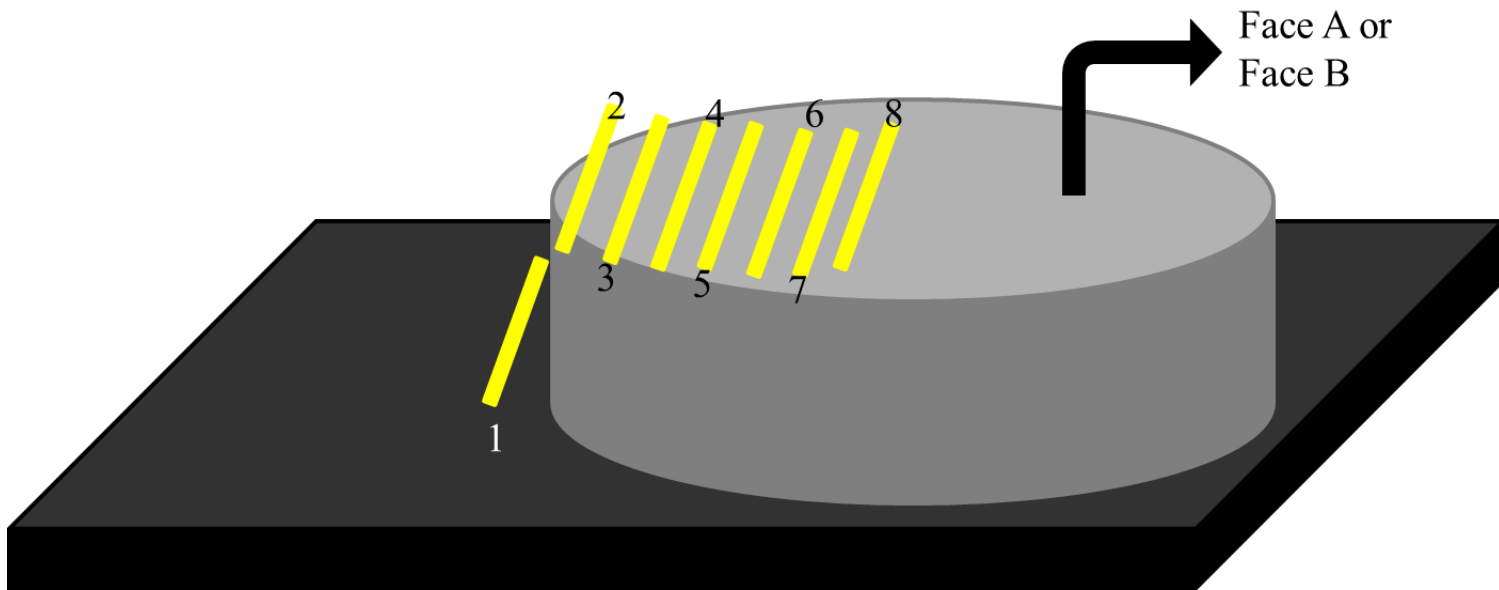


Fig. 12

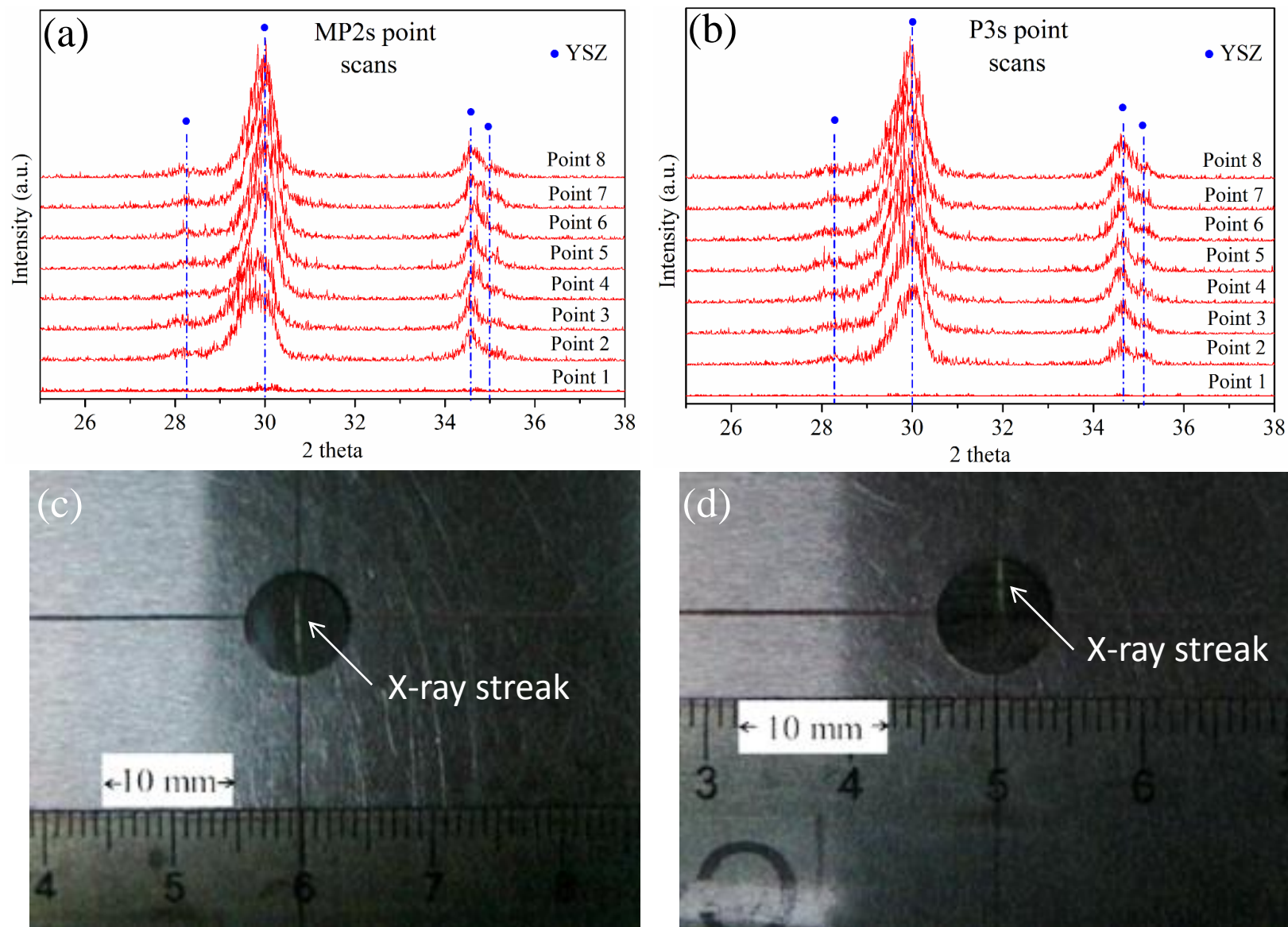


Fig. 13